Published as: *Nature*. 2010 December 9; 468(7325): 844–847.

# Design, function, and structure of a monomeric CLC transporter

**Janice L. Robertson**, **Ludmila Kolmakova-Partensky**, and **Christopher Miller**
Department of Biochemistry, Howard Hughes Medical Institute, Brandeis University, Waltham, Massachusetts 02454

## Abstract

Channels and transporters of the CLC family bring about transmembrane movement of inorganic anions in service of a variety of biological tasks, from the arcane - generating the kilowatt pulses by which electric fish parboil their prey - to the quotidian - acidification of endosomes, vacuoles, and lysosomes1. The homodimeric architecture of CLC proteins (Fig 1), initially inferred from single-molecule studies of an elasmobranch $Cl^-$ channel2 and later confirmed by crystal structures of bacterial $Cl^-/H^+$ antiporters3,4, appears to be universal. Moreover, the basic machinery enabling ion movement through these proteins - the aqueous pores for anion diffusion in the channels and the ion-coupling chambers that coordinate $Cl^-$ and $H^+$ antiport in the transporters - are contained wholly within each subunit of the homodimer. The near-normal function of a bacterial CLC transporter strait-jacketed by covalent crosslinks across the dimer interface and the behavior of a concatameric human homologue argue that the transport cycle resides within each subunit and does not require rigid-body rearrangements between subunits5,6. However, this evidence is only inferential, and since examples are known in which quaternary rearrangements of extramembrane CLC domains that contribute to dimerization modulate transport activity7, we cannot declare as definitive a “parallel pathways” picture in which the homodimer consists of two single-subunit transporters operating independently. A strong prediction of such a view is that it should in principle be possible to obtain a monomeric CLC. In this study, we exploit the known structure of a CLC $Cl^-/H^+$ exchanger, CLC-ec1 from E. coli, to design mutants that destabilize the dimer interface while preserving both structure and transport function of individual subunits. The results demonstrate that the CLC subunit alone is the basic functional unit for transport and that cross-subunit interaction is not required for $Cl^-/H^+$ exchange in CLC transporters.

---

To develop a strategy for generating a monomeric CLC, we examined the structure of CLC-ec1 for candidate-residues mediating dimerization. This homologue is well-suited to our purpose because its dimerization interface is almost completely membrane-embedded, the large intracellular C-terminal domain found in some CLCs being absent here. The interface is mainly formed by four helices running roughly perpendicular to the membrane to create a flat, nonpolar surface of ~1200 $X^2$ (Fig 1). Most cross-subunit contacts are made by interdigitated leucine and isoleucine sidechains; residues capable of forming hydrogen bonds or salt bridges are absent. The protein’s phospholipid-facing residues are also

---



**Author contributions:** Experiments were designed by JLR and CM and carried out by JLR and LKP, and the manuscript was written by all authors. Structure of the WW monomer is deposited as PDB # 3NMO.

nonpolar (Fig 1), a circumstance that invites questions of how such chemically similar surfaces so faithfully choose their respective protein and lipid partners in the dimer. Such questions have motivated extensive studies of transmembrane peptide dimerization8–10, which identified shape-complementarity as an important determinant of helix packing specificity within membranes and micelles. Shape-complementarity of the CLC-ec1 dimer interface is high, scoring at levels seen for protein-antibody contacts and several membrane protein oligomers (Supplementary Table 1). Accordingly, our design strategy seeks to destabilize the dimer by placing steric mismatches on the CLC subunit-interface. A second element of the strategy aims at favoring the interface's exposure to the lipid bilayer. Lipid-facing surfaces of many membrane proteins are known to present amphiphilic tryptophan or tyrosine sidechains to the chemically heterogeneous transition zone where the lipid acyl chains connect to the polar headgroups, as seen for CLC-ec1 in Fig 1; membrane-thermodynamic analysis of tryptophan analogues establishes that the aromatic, bifunctional character of this sidechain favors its location at the phospholipid bilayer's transition zone11.

With these considerations in mind, we adopted a "warts-and-hooks" strategy for engineering a monomeric CLC by introducing tryptophan mutations on the subunit interface near the level of the lipid headgroups. This type of substitution simultaneously offers two kinds of perturbation: (1) steric disruption of the contact surface's shape-complementarity and (2) enhanced affinity of this surface for the lipid bilayer. Eight single tryptophan substitutions for leucine or isoleucine were constructed near the extracellular and intracellular ends of the four dimerization helices (Figure 2a). All but one of these mutants express near wildtype levels, and the oligomerization state for each was analyzed in decylmaltoside (DM) micelles on a size exclusion column calibrated by a panel of membrane transport proteins12 (Fig 2b). The wildtype homodimer (100 kDa) elutes, as expected, at 12.8 mL, while the 50-kDa monomer is predicted to elute about 1 mL later. One mutant, I422W, shifts precisely to the presumed monomer position, with a minor dimer peak also apparent. Three other mutants, I201W, L406W and L434W, show broader, asymmetric peaks centered between dimer and monomer positions. The remaining three mutants all run as dimers (data not shown). In hopes of further stabilizing a monomer, we tested the double mutant I201W/I422W, which if dimeric would place four "warts" within the subunit contact region or, if monomeric, would offer two "hooks" to the bilayer, one on each side of the membrane. This mutant, henceforth denoted "WW," cleanly shifts to the monomer position with no observable dimer peak. The oligomeric nature of the double mutant in detergent micelles was further assessed by treatment with glutaraldehyde, a promiscuous crosslinker known to quantitatively produce covalent dimer of CLC-ec113, as illustrated for wildtype on the SDS-PAGE gels of Fig 2c. In contrast, glutaraldehyde treatment fails to shift WW to the covalent-dimer position, thereby identifying it as an isolated monomer in detergent.

To identify the oligomeric state of WW in lipid bilayers, we repeated glutaraldehyde crosslinking experiments on this protein reconstituted into liposomes. Phosphatidylcholine/phosphatidylglycerol (PC/PG) mixtures were used here to avoid lipid-associated amino groups that would confound the glutaraldehyde reaction. We also aimed in these experiments to approximate Poisson-dilution conditions14, wherein a low protein/lipid ratio is used so that most liposomes are protein-free, and any liposome containing protein carries only a single transporting unit. Under such conditions, each liposome becomes a single-

molecule reaction vessel in which intramolecular crosslinking is favored. As shown in Fig 3a, crosslinking in liposomes recapitulates the detergent results, thereby showing that WW is also monomeric in these bilayer membranes.

The experiments above establish the WW mutant as monomeric but do not speak to its conformational or functional character. We therefore performed two mechanistically diagnostic ion-transport measurements in the same liposome environment used for the crosslinking experiments. The unitary passive $Cl^-$ transport rate was determined in a "$Cl^-$ dump" experiment14, in which liposomes loaded with high $Cl^-$ are suspended in low-$Cl^-$ solution in the presence of $H^+$ and $K^+$ ionophores, to prevent a pH gradient buildup and to maintain zero voltage. Under these conditions, the unitary $Cl^-$ efflux rate of wildtype protein, measured electrochemically by appearance of $Cl^-$ in the external solution (Fig 3b), is ~300 $s^{-1}$; $Cl^-$ turnover by WW is roughly half of this value (160 $s^{-1}$), a respectable activity. Furthermore, anion specificity of transport is maintained in WW, since $Cl^-$ efflux is fully dependent on addition of $K^+$ ionophore. CLC-ec1 is a coupled $Cl^-/H^+$ exchanger, in which a pre-established $Cl^-$ gradient can be used to pump $H^+$ thermodynamically uphill15. The WW monomer retains this defining feature of the transport mechanism. As shown in Fig 3c, $Cl^-$-loaded liposomes are suspended in low-$Cl^-$ medium, and transport is initiated by depolarizing the liposomes with $K^+$-ionophore. As $Cl^-$ flows out, $H^+$ enters against a pH gradient, as detected by alkalinization of the extraliposomal medium, which is swiftly reversed by addition of a proton ionophore. $Cl^-/H^+$ exchange stoichiometry was estimated from the ratio of initial flux rates (Supplementary Fig 1): 2.1 ± 0.3 for wildtype control, as expected from the 2-to-1 stoichiometry determined in E. coli lipids14–16, and a similar value, 2.3 ± 0.3, for WW. The preservation of $H^+$-coupled $Cl^-$ antiport in the monomeric construct directly establishes that the CLC subunit itself contains all essential components of the transport mechanism. Of course, the possibility remains that sidechain movements at the dimer interface in wildtype homodimer may occur during the transport cycle, as indicated convincingly by recent $^{19}$F-NMR experiments17, but our results demonstrate that such movements cannot represent functionally obligatory cross-subunit interactions.

We crystallized the WW mutant, collected x-ray diffraction data to 3.1X, and solved the structure by molecular replacement using the wildtype subunit as search model (crystallographic statistics in Supplementary Table 2). The asymmetric unit consists of a single monomer whose previously buried dimer interface is now completely exposed to detergent-containing solvent. This exposed interface is shown (Fig 4a, Supplementary Fig 2) for a symmetry-related pair of monomers, whose contacts in the unit cell arise from crystal geometry and are not seen in crystals of wildtype CLC-ec1. We consider it remarkable that the monomer's 18 membrane-embedded helices align precisely with those of the wildtype subunit in the homodimer (Fig 4b), despite the absence of native cross-subunit interactions. Only the cytoplasmic N-terminal helix (residues 22–30), which in the wildtype engages in a domain-swap with its twin subunit, veers off in a different direction to accommodate crystal packing. Moreover, most sidechains projecting from the exposed subunit interface are well-ordered and unperturbed from their buried positions in the wildtype dimer, except for a single tyrosine, which adopts a different rotamer to make room for one of the substituted tryptophans (Supplementary Fig. 3). Unambiguous density for the mechanistically crucial central $Cl^-$ ion appears in the monomer at the same position as in wildtype, coordinated by

the central serine and tyrosine residues (Fig 4, Supplementary Fig 2); however, $Cl^-$ density is weaker in WW than in wildtype datasets of similar crystallographic quality18, perhaps because crystallization of the monomer requires the additional presence of $NO_3^-$, a transported anion known to compete with $Cl^-$13,19.

A perplexing clash of form and function arises from this demonstration that the isolated CLC subunit is transport-competent. Why then are all known CLC proteins homodimers? With the steady expansion of the membrane protein structural database, it is becoming apparent that the parallel-pathways theme discussed here for CLCs appears in many families of channels and transporters. For instance, aquaporin channels are homotetramers with a diffusion pore in each subunit20, while FNT-family formate channels are five-pore pentamers21,22, and UT urea channels23, Amt-type ammonia channels24,25, and outer membrane porins26 are three-pore trimers. Among membrane transporters, a striking example is found in five phylogentically unrelated families whose transporting subunits share a common structural fold but variously assemble as monomers, dimers, or trimers27,28. A survey of current literature identifies no fewer than fourteen separate families (~ 40% of structurally known membrane-transport protein families) built on this parallel-pathway principle, with subunits held together through extended, nonpolar intramembrane contacts. We are loath to offer any suggestion for the “meaning”-evolutionary or physiological - of this emerging structural theme; in only one case, a trimeric $Na^+$-coupled aspartate transporter of the EAAT superfamily29, has parallel-pathway architecture been plausibly proposed as essential for substrate transport by the individual subunits making up the complex.

Although our warts-and-hooks design succeeded in severing the CLC dimer, we do not claim to understand the thermodynamic reasons for its success. The energetic components governing how a greasy protein surface chooses its greasy protein partner over a greasy lipid bilayer are still unparsed. Previous attempts to attack this fundamental problem of membrane protein chemistry have focused upon model systems of single transmembrane helical peptides8–10,30, and most have been quantifiable only in detergent micelles. The CLC interface introduced here may provide future opportunities to examine the molecular forces operating in transmembrane helix packing, folding, and recognition in the context of a complex integral membrane protein.

## Methods Summary

Expression in E. coli, purification, and liposome reconstitution of CLC-ec1 (Swiss-Prot ID P37019) were performed as described14, as were $Cl^-$ and $H^+$ flux assays, except that we used lipid mixtures of egg phosphatidylcholine and 1-palmitoyl, 2-oleoyl phosphatidylyglycerol, 3/1 weight ratio. Ion flux rates in these lipids are 5–10-fold lower than observed in the E. coli phospholipids that we customarily use. Liposomes were formed at 20 mg/mL lipid, 1 μg protein/mg lipid by dialysis or by centrifugation of 0.1 mL samples through 3-mL Sephadex G-50 columns. $Cl^-/H^+$ exchange stoichiometry was determined as the ratio of initial transport rates16, with $Cl^-$ efflux and $H^+$ uptake recorded via $Cl^-$ and $H^+$ electrodes using liposomes loaded with 300 mM KCl, 40 mM citrate-NaOH pH 5.0 suspended in solutions of 1 mM KCl, 300 mM K-isethionate, 2 mM citrate-NaOH pH 5.2.

For crystallography, CLC protein (9–15 mg/mL) in 100 mM NaCl, ~40 mM DM,10 mM tris-HCl pH 7.5 was mixed with an equal volume of 100 mM $LiNO_3$, 41–45% (w/v) PEG400, 100 mM glycine-NaOH pH 9.5, with ~10 mM 4-cyclohexyl-1-butyl-β-D-maltoside added to the 2 μL drop. Crystals grown by vapor diffusion in sitting drop trays for 2–4 weeks at 20°C were frozen in liquid nitrogen, and data were collected remotely at beamline 8.2.1, Advanced Light Source Eastern Annex, Waltham, Mass. Data were processed in HKL2000. Molecular replacement was done in PHASER using residues 30–450 of a single subunit of CLC-ec1 as search model, and refinement was carried out in Refmac5.

## Supplementary Material

Refer to Web version on PubMed Central for supplementary material.

## Acknowledgments

We are grateful to the scientists at beamline 8.2.1, Advanced Light Source, Lawrence Berkeley Laboratory, for much skilled help and advice, to Dr H. Jayaram for help with refinement, and to Drs R. Sah and D. Theobald for comments on the manuscript. Supported in part by N.I.H. grant GM31768.

## References

1. Jentsch TJ, Poet M, Fuhrmann JC, et al. Physiological functions of CLC Cl-channels gleaned from human genetic disease and mouse models. Annu Rev Physiol. 2005; 67:779–807. [PubMed: 15709978]
2. Middleton RE, Pheasant DJ, Miller C. Reconstitution of detergent-solubilized $Cl^-$ channels and analysis by concentrative uptake of $^{36}Cl^-$ and planar lipid bilayers. Methods. 1994; 6:28–36.
3. Dutzler R, Campbell EB, Cadene M, et al. X-ray structure of a ClC chloride channel at 3.0 A reveals the molecular basis of anion selectivity. Nature. 2002; 415:287–294. [PubMed: 11796999]
4. Dutzler R, Campbell EB, MacKinnon R. Gating the selectivity filter in ClC chloride channels. Science. 2003; 300:108–112. [PubMed: 12649487]
5. Nguitragool W, Miller C. CLC $Cl^-/H^+$ transporters constrained by covalent cross-linking. Proc Natl Acad Sci USA. 2007; 104:20659–20665. [PubMed: 18093952]
6. Zdebik AA, Zifarelli G, Bergsdorf EY, et al. Determinants of anion-proton coupling in mammalian endosomal CLC proteins. J Biol Chem. 2008; 283:4219–4227. [PubMed: 18063579]
7. Bykova EA, Zhang XD, Chen TY, et al. Large movement in the C terminus of CLC-0 chloride channel during slow gating. Nature Struct Mol Biol. 2006; 13:1115–1119. [PubMed: 17115052]
8. Fleming KG, Ackerman AL, Engelman DA. The effect of point mutations on the free energy of transmembrane a-helix dimerization. J Mol Biol. 1997; 272:266–275. [PubMed: 9299353]
9. MacKenzie KR, Fleming KG. Association energetics of membrane spanning alpha-helices. Curr Opin Struct Biol. 2008; 18:412–419. [PubMed: 18539023]
10. Chen L, Merzlyakov M, Cohen T, et al. Energetics of ErbB1 transmembrane domain dimerization in lipid bilayers. Biophys J. 2009; 96:4622–4630. [PubMed: 19486684]
11. Yau WM, Wimley WC, Gawrisch K, et al. The preference of tryptophan for membrane interfaces. Biochemistry. 1998; 37:14713–14718. [PubMed: 9778346]
12. Fang Y, Kolmakova-Partensky L, Miller C. A bacterial arginine-agmatine exchange transporter involved in extreme Acid resistance. J Biol Chem. 2007; 282:176–182. [PubMed: 17099215]
13. Maduke M, Pheasant DJ, Miller C. High-level expression, functional reconstitution, and quaternary structure of a prokaryotic ClC-type chloride channel. J Gen Physiol. 1999; 114:713–722. [PubMed: 10539975]
14. Walden M, Accardi A, Wu F, et al. Uncoupling and turnover in a $Cl^-/H^+$ exchange transporter. J Gen Physiol. 2007; 129:317–329. [PubMed: 17389248]

15. Accardi A, Miller C. Secondary active transport mediated by a prokaryotic homologue of ClC Cl-channels. Nature. 2004; 427:803–807. [PubMed: 14985752]
16. Miller C, Nguitragool W. A provisional transport mechanism for a CLC-type $Cl^-/H^+$ exchanger. Phil Trans Roy Soc B. 2008
17. Elvington SM, Liu CW, Maduke MC. Substrate-driven conformational changes in ClC-ec1 observed by fluorine NMR. Embo J. 2009; 28:3090–3102. [PubMed: 19745816]
18. Accardi A, Lobet S, Williams C, et al. Synergism between halide binding and proton transport in a CLC-type exchanger. J Mol Biol. 2006; 362:691–699. [PubMed: 16949616]
19. Nguitragool W, Miller C. Uncoupling of a CLC $Cl^-/H^+$ exchange transporter by polyatomic anions. J Mol Biol. 2006; 362:682–690. [PubMed: 16905147]
20. Fu D, Libson A, Miercke LJ, et al. Structure of a glycerol-conducting channel and the basis for its selectivity. Science. 2000; 290:481–486. [PubMed: 11039922]
21. Wang Y, Huang Y, Wang J, et al. Structure of the formate transporter FocA reveals a pentameric aquaporin-like channel. Nature. 2009; 462:467–472. [PubMed: 19940917]
22. Waight AB, Love J, Wang DN. Structure and mechanism of a pentameric formate channel. Nature Struct Mol Biol. 2010; 17:31–37. [PubMed: 20010838]
23. Levin EJ, Quick M, Zhou M. Crystal structure of a bacterial homologue of the kidney urea transporter. Nature. 2009; 462:757–761. [PubMed: 19865084]
24. Khademi S, O'Connell J 3rd, Remis J, et al. Mechanism of ammonia transport by Amt/MEP/Rh: structure of AmtB at 1.35 A. Science. 2004; 305:1587–1594. [PubMed: 15361618]
25. Zheng L, Kostrewa D, Berneche S, et al. The mechanism of ammonia transport based on the crystal structure of AmtB of Escherichia coli. Proc Natl Acad Sci USA. 2004; 101:17090–17095. [PubMed: 15563598]
26. Cowan SW, Schirmer T, Rummel G, et al. Crystal structures explain functional properties of two E. coli porins. Nature. 1992; 358:727–733. [PubMed: 1380671]
27. Shaffer PL, Goehring A, Shankaranarayanan A, et al. Structure and mechanism of a Na+-independent amino acid transporter. Science. 2009; 325:1010–1014. [PubMed: 19608859]
28. Theobald DL, Miller C. Membrane transport proteins: surprises in structural sameness. Nature Struct Mol Biol. 17:2–3. [PubMed: 20051980]
29. Reyes N, Ginter C, Boudker O. Transport mechanism of a bacterial homologue of glutamate transporters. Nature. 2009; 462:880–885. [PubMed: 19924125]
30. Metcalf DG, Kulp DW, Bennett JS, et al. Multiple approaches converge on the structure of the integrin alphaIIb/beta3 transmembrane heterodimer. J Mol Biol. 2009; 392:1087–1101. [PubMed: 19527732]

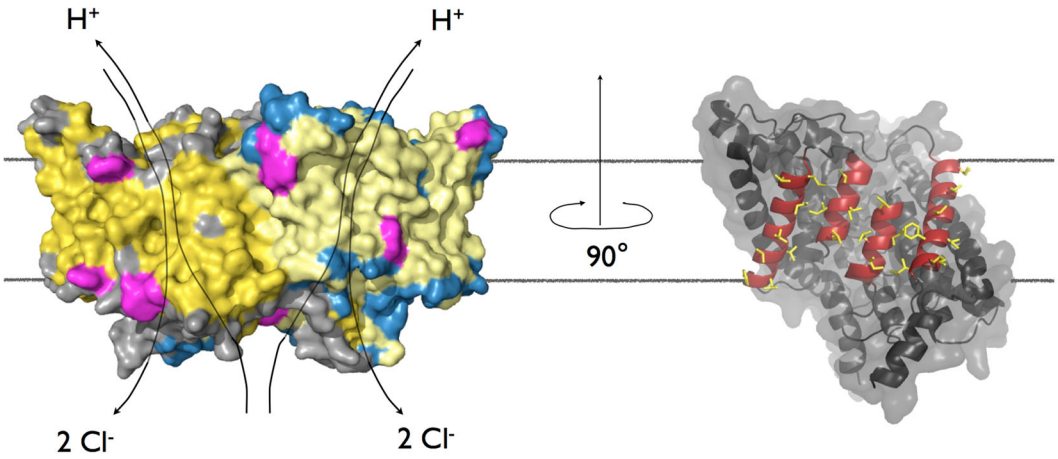


**Figure 1. Structure and dimeric interface of ClC-ec1**

Left panel: ClC-ec1 dimer (PDB: 1OTS) is shown with subunits in grey and blue, with hydrophobic residues highlighted in yellow and tryptophan, tyrosine in magenta. Level of the membrane (extracellular side up) is indicated by black lines. Previously proposed transport pathways[31] are shown for $Cl^-$ and $H^+$. Right panel: single subunit rotated 90° to view the dimerization interface head-on. The four interface helices (residues 192–204, 215–232, 405–416, 422–440) are shown in red and sidechains involved in cross-subunit contacts in yellow.

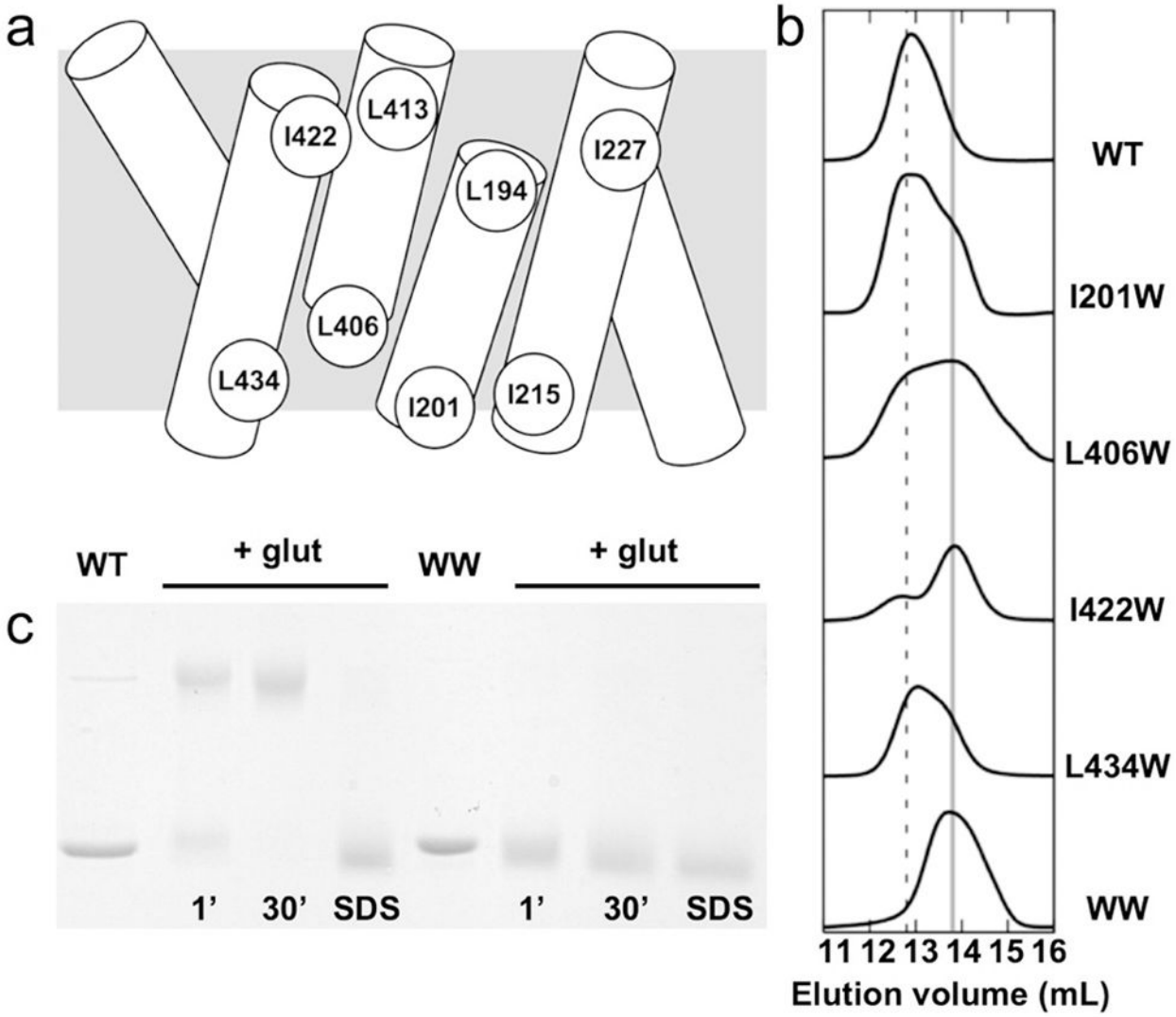


**Figure 2. Behavior of tryptophan mutants in detergent**

a. A schematic of the dimerization interface showing positions of tryptophans tested. L194W did not express protein. b. Chromatographic profiles of the various mutants on Superdex 200. Vertical lines mark elution volumes for dimer and monomer. c. 10% SDS-PAGE of wildtype and WW samples, coomassie stained. Bars indicate samples at 0.25 mg/mL treated with 0.125% glutaraldehyde, 150 mM NaCl, 50 mM Na-phosphate pH 7.0 for the indicated times in 5 mM decylmaltoside or, as a negative control, in 2% SDS. Note that crosslinking is nearly complete in 1 minute, and that no higher oligomers appear even at 30 min.

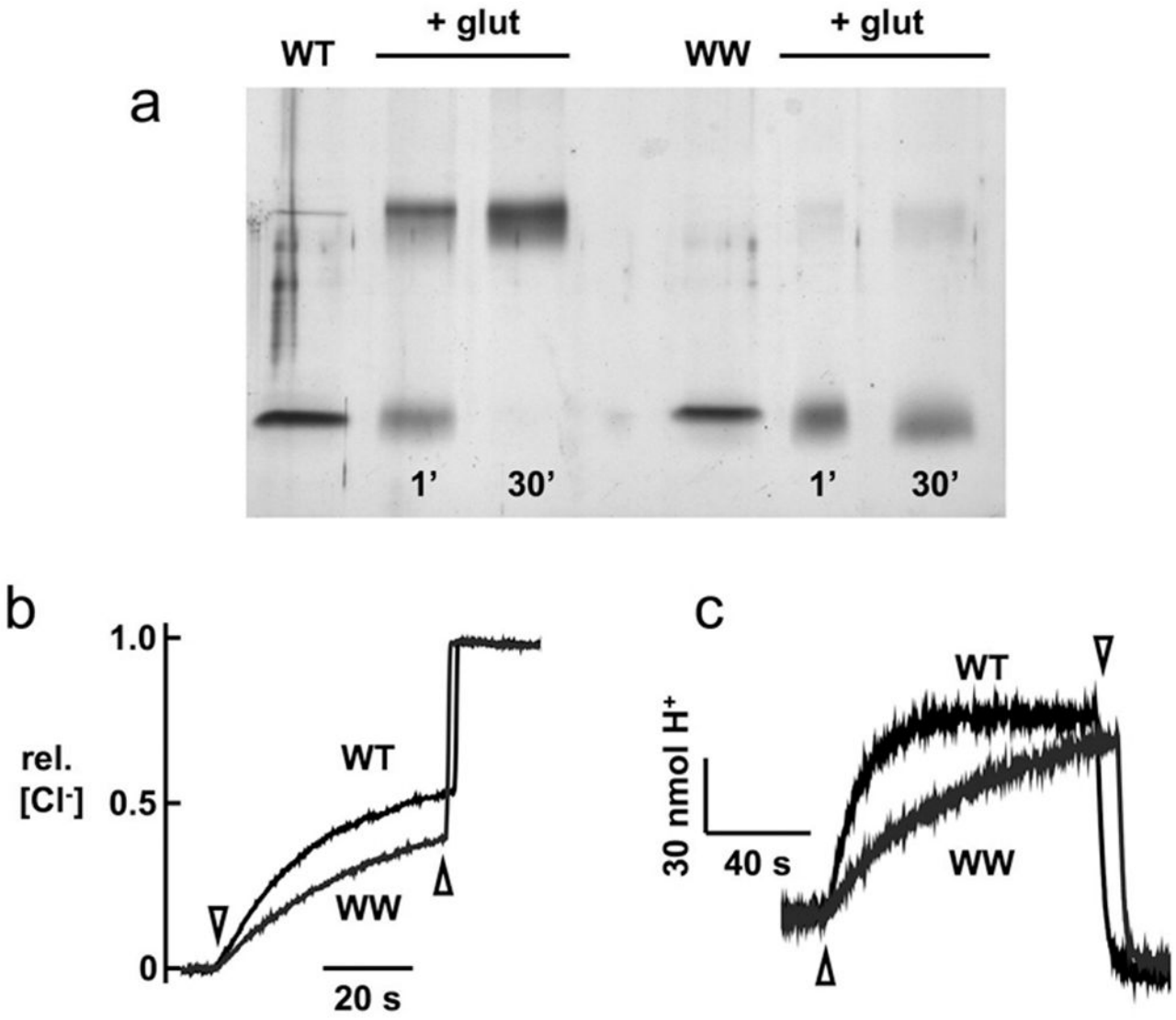


**Figure 3. Monomeric CLC mutant in phospholipid membranes**

a. Glutaraldehyde crosslinking of wildtype ClC-ec1 and WW mutant in liposomes. Glutaraldehyde treatment was as in Fig 2, except that protein was incorporated into PC/PG liposomes, and gel was silver-stained. b. Passive $Cl^-$ efflux from reconstituted liposomes for wildtype ClC-ec1 and WW mutant. Traces show release of $Cl^-$ from liposomes loaded with 300 mM $Cl^-$ into the extraliposomal solution (containing 1 mM $Cl^-$) initiated by 0.5 μM valinomycin (downward arrow), normalized to the level of complete release upon disrupting liposomes with 50 mM octylglucoside (upward arrow). Unitary turnover calculated on a per-subunit basis from the initial rate of $Cl^-$ release14 was: 290 ± 30 $s^{-1}$ for wildtype, 160 ± 9 $s^{-1}$ for WW (mean ± s.e.m, N=9). c. $Cl^-$-driven $H^+$ pumping against a pH gradient. Liposomes loaded with 300 mM $Cl^-$ pH 5.0, were suspended in 1 mM $Cl^-$, pH 5.2, and transport was initiated by valinomycin and terminated by FCCP (arrows), while pH of suspension was recorded. Upward deflection represents uptake of $H^+$ into liposomes.

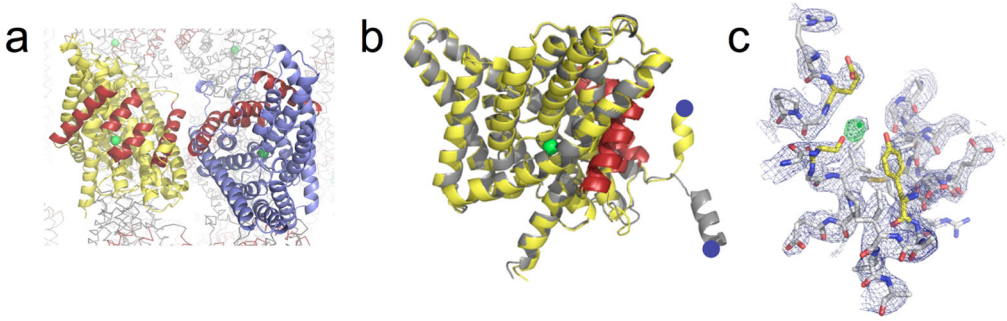


**Figure 4. Crystal structure of WW monomer**

a. View of two monomers in side-by-side contact, with interface helices highlighted in red, $Cl^-$ ion in green, and additional symmetry-related monomers in the background (grey). b. Backbone alignment (Cα r.m.s.d. 0.6 X) of WW monomer (yellow, with interface helices in red) with a single subunit of wildtype CLC-ec1 (grey). Blue spheres indicate the N-termini of the visible structures. c. Central anion-binding site. 2Fo-Fc map (blue, 1.5 σ) is shown near the central $Cl^-$-binding site, with coordinating residues Ser107, Glu148, and Tyr445 highlighted (yellow); positive difference density calculated from a $Cl^-$-omit map (green) shows a strong peak (3.5 σ) at the position of the central $Cl^-$ ion in wildtype. Stereo versions of panels **a** and **c** are displayed in Supplementary Fig 2.